

Procedure for determining activity concentrations of radionuclides due to elevated artificial gross gamma activity concentration

D- γ -GESAMT-MWASS-02

Authors:

M. Martens

M. Grüttmüller

K. Becker

S. Schmied

C. Wedekind

G. Kanisch

Federal coordinating office for seawater,
suspended particulate matter and sediment
(Leitstelle für Meerwasser, Meeresschwebstoff und-sediment)

Procedure for determining activity concentrations of radionuclides due to elevated artificial gross gamma activity concentration

1 Scope

The procedure outlined in the following is used if the threshold value of the artificial gross gamma activity concentration of $1\,000\text{ Bq}\cdot\text{m}^{-3}$, as described in the procedure D-γ-GESAMT-MWASS-01, is exceeded due to an increased input of artificial radionuclides. Individual radionuclides or radionuclide mixtures can be quickly identified qualitatively from the pulse height spectra obtained. If necessary, their activity concentrations can be estimated. For a more precise determination of the activity concentrations of radioactive substances in seawater, a method suitable for the respective incident must be used.

2 Sampling

For this procedure, sampling is not required.

3 Analysis

3.1 Principle of the procedure

With this integral procedure, the count rates resulting from the interaction of gamma radiation in seawater with thallium-doped sodium iodide detectors (NaI(Tl) detectors) are determined directly in a quasi-continuous way, viz. cyclically with a measurement duration of one hour.

The procedure allows the recording and evaluation of pulse height spectra in the form of hourly spectra, which can be summed up to daily or weekly spectra if required. Although the low energy resolution of the NaI(Tl) detectors allows only limited nuclide-specific evaluation, individual radionuclides such as caesium-137 (Cs-137) and accident-typical radionuclide mixtures can be detected and separated from natural radioactive substances on the basis of the different gamma radiation energies [1, 2, 3, 4].

3.2 Sample preparation

A sample preparation is not required.

3.3 Radiochemical separation

A radiochemical separation is not required.

4 Measuring the activity

4.1 General

For basic information, the procedure D- γ -GESAMT-MWASS-01 is to be considered.

In the pulse height spectra in Figure 1, in addition to the natural radionuclides from the uranium decay series and the K-40 in seawater of the Baltic Sea, Cs-137, most of which originated from the accident at the Chernobyl nuclear power plant, can also be seen.

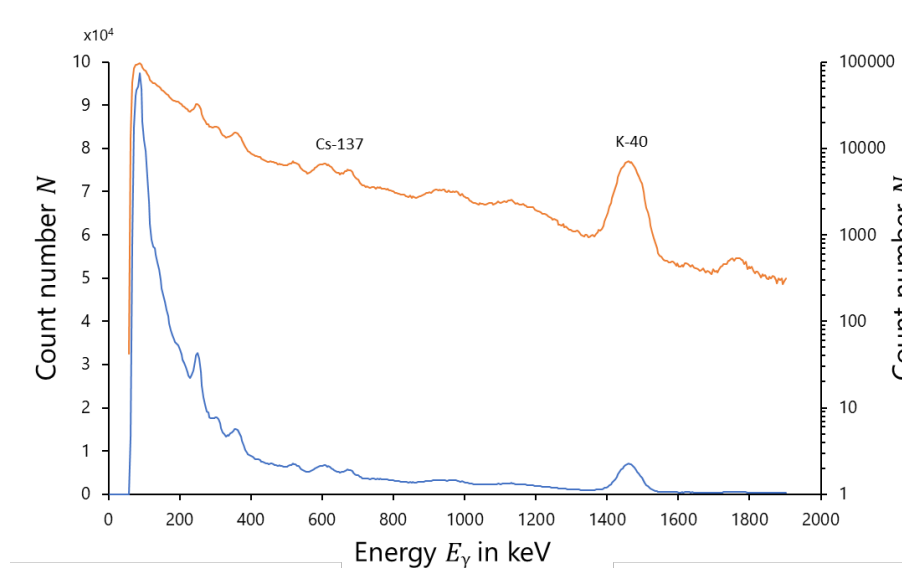


Fig. 1: Example of a weekly spectrum of the station Kühlungsborn. The calibration of the spectrum (blue: y-axis linear, red: y-axis logarithmic) was done via K-40.

For nuclide-specific statements from such readily identifiable gamma peaks, the spectrometric detection efficiency $\varepsilon_{Sp}(E_\gamma)$ of the measuring device is required. From this, the nuclide-specific detection efficiency $\varepsilon_{SpN}(E_\gamma)$ is derived to calculate the activity concentration.

4.2 Calibration

4.2.1 Experimental calibration

The experimental calibration of the spectrometric detection efficiency $\varepsilon_{Sp}(E_\gamma)$ is not reasonably possible for the measurement arrangement "probe in the vessel's strom box". Therefore, the present procedure shall only be used for the measurement arrangement "probe hanging freely in the water". The calibration for this measurement arrangement is described in Annex A.2 of the procedure D- γ -GESAMT-MWASS-01.

The spectrometric detection efficiency $\varepsilon_{\text{Sp}}(E_\gamma)$ for a selected radionuclide with a metrologically traceable activity concentration c , a count number N_{Sp} , and a measurement duration t_m is calculated according to Equation (1):

$$\varepsilon_{\text{Sp}}(E_\gamma) = \frac{N_{\text{Sp}}}{c \cdot p_\gamma \cdot t_m} \quad (1)$$

The nuclide-specific detection efficiency $\varepsilon_{\text{SpN}}(E_\gamma)$ is obtained by multiplying the gamma peak emission intensity p_γ according to Equation (2):

$$\varepsilon_{\text{SpN}}(E_\gamma) = \varepsilon_{\text{Sp}}(E_\gamma) \cdot p_\gamma \quad (2)$$

4.2.2 Calibration via Monte Carlo simulation

Due to the large effort of experimental calibration, the detection efficiency ε_{Sp} for in situ measurement in seawater is preferably carried out with Monte Carlo simulation [5, 6, 7]. Using the algorithms described in the PENELOPE report [8], an application was programmed to calculate the detection efficiency of a NaI(Tl) detector, where the NaI(Tl) crystal is surrounded by a waterproof polyamide (Ertalon® 6 xau) case of 8 mm thickness. The detector is located in the center of a water sphere. The radius depends on the gamma energy and ranges from 31 cm for 50 keV to 146 cm for 2000 keV (sphere volumes from 0,12 m³ to 13 m³).

The resulting energy-dependent spectrometric detection efficiency is shown in Figure 2.

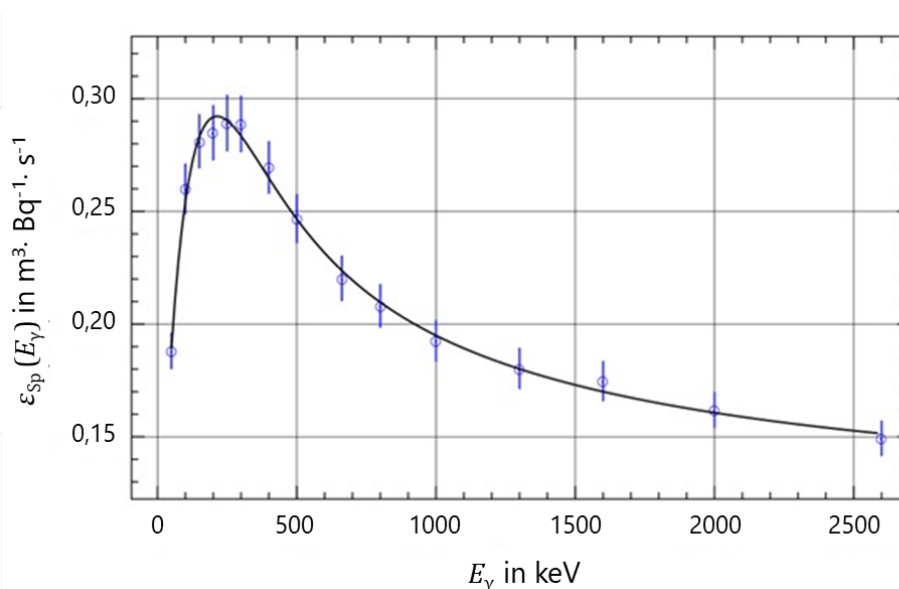


Fig. 2: Energy-dependent spectrometric detection efficiency $\varepsilon_{\text{Sp}}(E_\gamma)$ obtained with MC simulation (blue boxes) and the (solid) curve of a polynomial fitted with six coefficients to the values as a function of $\ln(E_\gamma)$.

The spectrometric detection efficiencies $\varepsilon_{Sp}(E_{\gamma})$ for calculating the nuclide-specific detection efficiency $\varepsilon_{SpN}(E_{\gamma})$ of a selection of relevant radionuclides is summarised in Table 1.

Tab. 1: Calibration data for selected radionuclides for the measurement arrangement "probe hanging freely in the water"

radionuclide data [9]		spectrometric detection efficiency (gamma peak efficiency)*	
radionuclide	E_{γ} in MeV	p_{γ}	ε_{Sp} in $m^3 \cdot Bq^{-1} \cdot s^{-1}$
K-40	1,46	0,11	$0,17 \cdot 10^{-3}$
Mn-54	0,83	1,0	$0,21 \cdot 10^{-3}$
Zn-65	1,12	0,50	$0,19 \cdot 10^{-3}$
Ru-106	0,51	0,21	$0,24 \cdot 10^{-3}$
	0,62	0,10	$0,23 \cdot 10^{-3}$
	1,06	0,015	$0,19 \cdot 10^{-3}$
I-131	0,36	0,81	$0,27 \cdot 10^{-3}$
	0,64	0,07	$0,23 \cdot 10^{-3}$
Cs-134	0,60	0,98	$0,23 \cdot 10^{-3}$
	0,80	0,85	$0,21 \cdot 10^{-3}$
	0,57	0,16	$0,24 \cdot 10^{-3}$
Cs-137	0,66	0,85	$0,22 \cdot 10^{-3}$
Ce-144	0,13	0,11	$0,27 \cdot 10^{-3}$

* calculated via Monte Carlo simulation

4.3 Measurement

For basic information, the procedure D- γ -GESAMT-MWASS-01 is to be considered.

4.4 Interferences

Due to the low energy resolution of the NaI(Tl) detectors used, overlaps of gamma peaks of different radionuclides, so-called multiplets, often occur. In Figure 3, a multiplet in the channel range b from 135 to 172 consisting of the peaks of the natural radionuclides thallium-208 (Tl-208) and bismuth-214 (Bi-214) as well as the peak of the artificial radionuclide Cs-137 is shown [10]. The procedure for the evaluation of such a multiplet is described in Section 5.4 of the General Chapter γ -SPEKT/GRUNDL of this Procedures Manual.

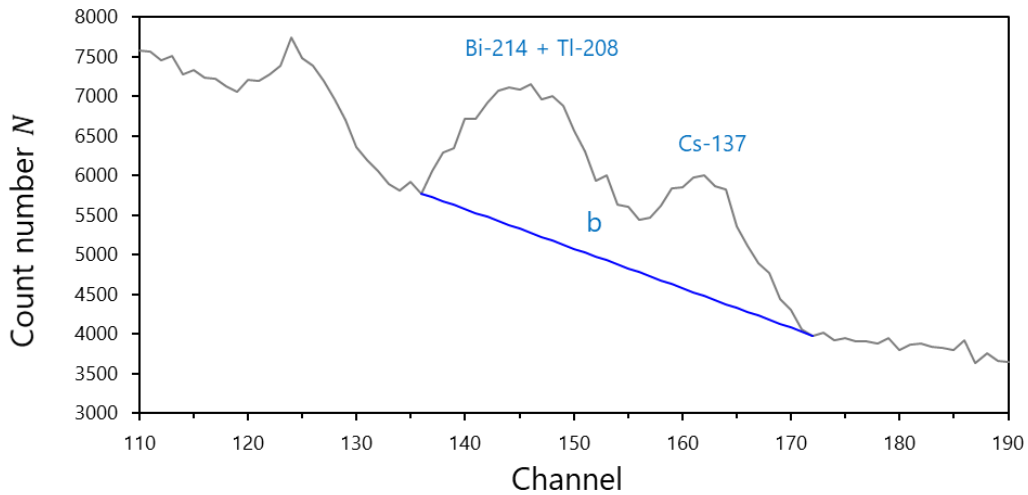


Fig. 3: Multiplet of peaks of the natural radionuclides Tl-208 and Bi-214 and the artificial radionuclide Cs-137 in the channel region b

For further information on interference, the General Chapter γ -SPEKT/INTERF of this Procedures Manual is to be considered.

5 Calculation of the results

5.1 Equations

If an undisturbed gamma peak is present in the NaI spectrum, the background contribution is determined using the trapezoidal method according to Section 5.3.1 of the General Chapter γ -SPEKT/GRUNDL of this Procedures Manual.

Since most of the peaks in the pulse height spectrum of a NaI(Tl) detector do not occur as single peaks but as multiplets (see Section 4.4), a least-squares method for peak fitting is used in the evaluation, which is described in Sections 5.3.3 and 5.4 of the General Chapter γ -SPEKT/GRUNDL of this Procedures Manual. Subsequently, a non-linear fit is carried out using the Levenberg-Marquardt method, in which the parameters initially held constant in the linear fit are also adjusted. The Excel data sheet used for fitting is shown in Figure 4, the pulse height spectrum together with resulting fit functions in Figure 5.

The activity concentration is calculated from the adjusted net peak areas by multiplication with a detector- and nuclide-specific calibration factor, viz. by using the detector detection efficiency and the gamma emission intensity of the considered radionuclide. Special explanations on the calculation of the output quantity and standard uncertainty using methods with linear deconvolution can be found in Section 4.2 and in Annex C.3 of the General Chapter CHAGR-ISO-01 of this Procedures Manual as well as in Table 7 of reference [11].

Note:

The influence of the water coverage does not come into effect in this case, since only net count rates are considered when evaluating with the linear spectrum deconvolution.

	A	B	C	D	E	F	G	H	I	J	K	L	M	N	O	P	Q	R	S	T	U	V
1	Kühlungsborn																					
2	08.02.2016 00:00																					
3				sigma=fwhm/2,355			Wert	sigf	u(pai)	urel(pai)	Wert	sigf	u(pai)	urel(pai)	Wert	sigf	u(pai)	urel(pai)	Wert	sigf	u(pai)	urel(pai)
4	Farblehre:	Eingabefelder	ROI-Anfangskanal	#kl			MP1				MP2				MP3				MP0			
5		NBA-Ausgabe	ROI-Endkanal	kr			63				105				313				0			
6		Excel_formeln	Messdauer in s	tm			104				187				392				0			
7			Anzahl UG-Parameter	nbg			86400				86400				86400				86400			
8			Breitenparameter, Kanal	sigma			3				3				3				3			
9			Parameter	tail			3.230				4.040				6.878				31.255			
10			1, 2 oder 3 UG-Parameter	ug1			3.972				11.196				31.255				3620.47			
11			Parameter	ug2			3620.17				4917.30				3620.47				-44.36			
12	#k_alpha	3		ug3			-44.35				25.10662				7.92866							
13	k_beta	1,645					7.93				125.954	0.915	511		350.820	1.000	1460,8					
14				1 bis 5 Peaklagenwerte, in Kanälen;	plage1		87.333	1.000	338,3		142.979	0.992	583,2		142.979	0.992	583,2					
15					plage2		0.971				149.920	1.018	609,3		149.920	1.018	609,3					
16					plage3		1.075				162.801	1.069	661,7		162.801	1.069	661,7					
17					plage4		1.105															
18					plage5																	
19				1 bis 5 Peakflächen, in Impulsen;	#pa1		5950,6		563,2	0,0947	1767,0		325,0	0,1839	18807,3		221,8	0,0118				
20					pa2				#DIV/0!		2281,2		370,4	0,1624			#DIV/0!					
21					pa3				#DIV/0!		2320,0		480,4	0,2071			#DIV/0!					
22					pa4				#DIV/0!		2736,7		353,6	0,1292			#DIV/0!					
23					pa5				#DIV/0!								#DIV/0!					
24				Auswahl Aktion																		
25									ChisqR:	7,663				ChisqR:	0,669				ChisqR:	0,709		
26																						
27				2. linear; 3. Parabel	#Ekal:										#Fwhm-Kal:							
28					npEK		3								hwb0 (keV)				-436,569			
29					e0 (keV)		-13,358		u(e0)	1,880					hwb1 (keV/keV)				4,1531			
30					e1 (keV/Kanal)		4,132		u(e1)	0,00699												
31					e2		0,00012703			0,00000												
32					#Efit_Pars																	
33					effp1-6		0,01237096	-0,0115	0,004124	-0,00071	5,8E-05	-1,849E-06										
34					eps = Polynom(ln(E(keV)))																	
35																						
36				spezielle Trennpunkte (Kanäle):			111															gelbe Zellen: enthalten Formeln!

Fig. 4: Structure of the Excel data sheet for the parameter defaults for fitting the model of the evaluation to the pulse height spectrum

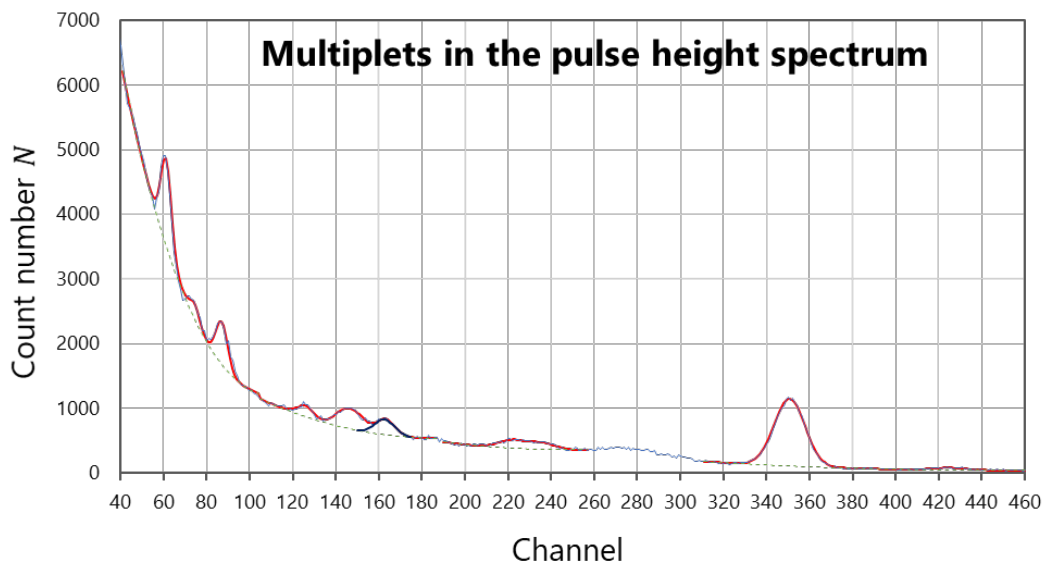


Fig. 5: Pulse height spectrum with resulting fit functions; light blue - measured pulse height spectrum; red - fit function; green dashed - background polynomial; dark blue - peak of the considered radionuclide Cs-137

5.1.1 Output quantity

According to Equation (3), the activity concentration c_r of the radionuclide r is calculated:

$$c_r = R_{n,r} \cdot \varphi_{SpN,r} \quad (3)$$

Herein are:

c_r activity concentration of the radionuclide r , in $\text{Bq}\cdot\text{m}^{-3}$;

$\varphi_{SpN,r}$ procedural calibration factor of the radionuclide r , in $\text{Bq}\cdot\text{s}\cdot\text{m}^{-3}$;

$$\varphi_{SpN,r} = \frac{1}{\varepsilon_{SpN}(E_\gamma)}$$

$\varepsilon_{SpN,r}$ nuclide-specific detection efficiency of the radionuclide r , in $\text{m}^3\cdot\text{Bq}^{-1}\cdot\text{s}^{-1}$;

$R_{n,r}$ net count rate of the considered gamma peak of the radionuclide r obtained from the peak fitting, in s^{-1} .

5.1.2 Standard uncertainty of the output quantity

The standard uncertainty $u(c_r)$ of the activity concentration of the radionuclide r is calculated according to Equation (4):

$$u(c_r) = c_r \cdot \sqrt{u_{\text{rel}}^2(\varphi_{SpN,r}) + \varphi_{SpN,r}^2 \cdot u^2(R_{n,r})} \quad (4)$$

where

$u(c_r)$ standard uncertainty of the activity concentration of the radionuclide r , in $\text{Bq}\cdot\text{m}^{-3}$;

$u_{\text{rel}}(\varphi_{SpN,r})$ relative standard uncertainty of the procedural calibration factor for the radionuclide r ;

$u(R_{n,r})$ standard uncertainty of the net count rate of the considered gamma peak of the radionuclide r , in s^{-1} .

5.2 Worked example

A worked example cannot be carried out here, since the underlying equations are too complex for a manual calculation. For the required non-linear spectrum deconvolution, an Excel VBA application is used (see Figure 4) [11].

5.3 Consideration of the uncertainties

The standard uncertainty of the analysis result includes the contributions of the counting statistics, the calibration, the emission intensity, and the location of the peak maxima. The standard uncertainty of the duration of measurement is neglected.

6 Characteristic limits of the procedure

The characteristic limits are calculated according to the ISO 11929 standard series [12]. Further considerations on the characteristic limits can be found in the General Chapter CHAGR-ISO-01 of this Procedures Manual.

For the procedure described above, the equations of the characteristic limits can only be solved computer-based.

6.1 Equations

6.1.1 Decision threshold

The decision threshold for the activity concentration c_r^* is determined using Equation (5):

$$c_r^* = k_{1-\alpha} \cdot \tilde{u}(0) \quad (5)$$

Herein are:

c_r^* decision threshold for the activity concentration of the radionuclide r , in $\text{Bq}\cdot\text{m}^{-3}$;

$k_{1-\alpha}$ quantile of the normal distribution for $\alpha = 0,0014$.

6.1.2 Detection limit

The detection limit for the activity concentration $c_r^\#$ is calculated according to the implicit Equation (6):

$$c_r^\# = c_r^* + k_{1-\beta} \cdot \tilde{u}(c_r^\#) \quad (6)$$

In Equation (6) are:

$c_r^\#$ detection limit for the activity concentration of the radionuclide r , in $\text{Bq}\cdot\text{m}^{-3}$;

$k_{1-\beta}$ quantile of the normal distribution for $\beta = 0,05$.

6.1.3 Limits of the coverage interval

The calculation of limits of the coverage interval are not required.

6.2 Worked example

A worked example cannot be carried out here, since the underlying equations are too complex for a manual calculation. For the calculation of the decision threshold and the detection limit, the Excel VBA application shown in Figure 4 is used [11].

7 Software supported calculation

7.1 View of the Excel spreadsheet

#	A	B	C	D	E	F	G	H	I	J	K	L	M	N	O	P	Q	R	S	T	U	V
1	Kühlungskern																					
2	08.02.2016 09:00			sigma=fwhm/2.355		Wert	sigf	u(pai)	urel(pai)		Wert	sigf	u(pai)	urel(pai)		Wert	sigf	u(pai)	urel(pai)		Wert	
3						MP1					MP2					MP3						MP0
4	Farblehre:	Eingabefelder	ROI-Anfangskanal	#Kl		63					105					313						0
5		YDA-Ausgabe	ROI-Endkanal	IR		104					187					392						0
6		Excel_Formeln	Messdauer in s	tm		86400					86400					86400						86400
7			Anzahl UG-Parameter	nbg		3					3					3						3
8			Breitenparameter, Kanal	sigma		3.230					4.040					6.878						
9			1, 2 oder 3 UG-Parameter	tail		3.972					11.196					31.255						
10				ug1		3620.17					4917.30					3620.47						
11				ug2		-44.35					-116.29					-44.36						
12	#k_alpha	3		ug3		7.93					25.10662					7.92866						
13	k_beta	1,645		1 bis 5 Peaklagewerte in Kanälen,	plage1	87,333	1,000	338,3			125,354	0,915	511			350,820	1,000	1460,8				
14					plage2	0,971					142,979	0,992	583,2			0,992						
15					plage3	1,075					149,920	1,018	609,3			1,041						
16					plage4	1,105					162,801	1,069	661,7									
17					plage5																	
18					#pai1	5950,6		563,2	0,0947		1767,0		325,0	0,1839		18807,3		221,8	0,0118			
19					pa2				#DIV/0!		2281,2		370,4	0,1624					#DIV/0!			
20					pa3				#DIV/0!		2320,0		480,4	0,2071					#DIV/0!			
21					pa4				#DIV/0!		2736,7		353,6	0,1292					#DIV/0!			
22					pa5				#DIV/0!										#DIV/0!			
23					Auswahl Aktion																	
24									ChisqR:	7,663				ChisqR:	0,669				ChisqR:	0,709		
25																						
26																						
27																						
28																						
29																						
30																						
31																						
32																						
33																						
34																						
35																						
36																						
37																						
38																						
39																						
40																						
41																						
42																						
43																						
44																						
45																						
46																						
47																						

The associated Excel file is available on request from the federal coordinating office.

7.2 View of the UncertRadio result page

A corresponding UncertRadio project file is not available for this Procedures Manual.

8 Catalogue of the chemicals und equipment

8.1 Chemicals

For this procedure, no chemicals are required.

8.2 Equipment

The equipment corresponds to that of the procedure D-γ-GESAMT-MWASS-01.

References

- [1] Wedekind, C., Schilling, G., Grützmüller, M., Becker, K.: *Neues Messverfahren zur Überwachung der Radioaktivität des Meeres im Bundes-Messnetz des BSH*. In: Bundesministerium für Umwelt, Naturschutz und Reaktorsicherheit (ed.): 10. Fachgespräch zur Überwachung der Umweltradioaktivität, Hamburg, 28. – 30. April 1998.
- [2] Wedekind, C., Schilling, G., Grützmüller, M., Becker, K.: *Gamma-radiation monitoring network at sea*. Applied Radiation and Isotopes, 1999, Vol. 50 (4), S. 733-741.

-
- [3] Wedekind, C.: *γ -Ray Spectrometer Probe for the Measurement of Radioactive Pollution in the Sea*. Health Physics, 1973, Vol. 25 (1), S. 51-58.
- [4] Wedekind, C., Becker, K., Schilling, G., Grützmüller, M.: *Marine environmental radioactivity monitoring by "in-situ" γ -radiation detection*. Kerntechnik, 2000, Vol. 65 (4), S. 190-194.
- [5] Han, S. Y., Maeng, S., Lee, H. Y., Lee, S. H.: *Preliminary study on the detection efficiency and estimation of minimum detectable activity for a NaI(Tl)-based seawater monitoring system*. Journal of Environmental Radioactivity, 2020, Vol. 218, S. 106222.
- [6] Naumenko, A., Andrukhovich, S., Kabanov, V., Kabanau, D., Kurochkin, Y., Martsynkevich, B., et al.: *Autonomous NaI(Tl) gamma-ray spectrometer for in situ underwater measurements*. Nuclear Instruments and Methods in Physics Research Section A: Accelerators, Spectrometers, Detectors and Associated Equipment, 2018, Vol. 908, S. 97-109.
- [7] Bagatelas, C., Tsabaris, C., Kokkoris, M., Papadopoulos, C., Vlastou, R.: *Monte Carlo simulation of a NaI detector in the aquatic environment*. In: Hellenic Nuclear Physics Society (ed.): HNPS Proceedings, 2009.
- [8] NEA: *PENELOPE 2018: A code system for Monte Carlo simulation of electron and photon transport*. In: Agency, N. E. (ed.): Workshop Proceedings, Barcelona, Spain, 28.01. – 01.02., 2019, S. 420.
Available at: <https://www.oecd-ilibrary.org/content/publication/32da5043-en>.
- [9] Laboratoire National Henri Becquerel (LNHB): *Nucléide - Lara: Library for gamma and alpha emissions*. In: Atomic and Nuclear Data. Last Update 10.11.2022. Available at: <http://www.lnhb.fr/nuclear-data/module-lara/>. [Last access 22.11.2022].
- [10] Nies, H., van Eck, G. T. M., de Jong, E. J.: *Radionuclides*. In: Laane, R. W. P. M. (Hrsg.): Background Concentrations of Natural Compounds in Rivers, Sea Water, Atmosphere and Mussels. Den Haag (NL): 1992, S. 40-49.
- [11] Kanisch, G.: *Bestimmung von Aktivitätskonzentrationen mittels spektrometrischer Analyse von NaI(Tl)-Gammaspekten einer Unterwassersonde*. Bundesamt für Seeschifffahrt und Hydrographie Ed., 2022, p. 33. Personal communication.
- [12] Standard series ISO 11929:2019, *Determination of the characteristic limits (decision threshold, detection limit and limits of the coverage interval) for measurements of ionizing radiation — Fundamentals and application (Parts 1 to 3)*.